PROCEEDINGS A

rspa.royalsocietypublishing.org

Research

Cite this article: Basak A, Gupta A. 2015 A three-dimensional study of coupled grain boundary motion with junctions. *Proc. R. Soc. A* **471**: 20150127.
http://dx.doi.org/10.1098/rspa.2015.0127

Received: 24 February 2015
Accepted: 9 April 2015

Subject Areas:
mechanical engineering, materials science

Keywords:
incoherent interfaces, triple junction, coupled grain boundary motion, geometrical coupling factor, nanocrystalline materials

Author for correspondence:
Anurag Gupta
e-mail: ag@iitk.ac.in

A three-dimensional study of coupled grain boundary motion with junctions

Anup Basak and Anurag Gupta

Department of Mechanical Engineering, Indian Institute of Technology, Kanpur, Uttar Pradesh 208016, India

A novel continuum theory of incoherent interfaces with triple junctions is applied to study coupled grain boundary (GB) motion in three-dimensional polycrystalline materials. The kinetic relations for grain dynamics, relative sliding and migration of the boundary and junction evolution are developed. In doing so, a vectorial form of the geometrical coupling factor, which relates the tangential motion at the GB to the migration, is also obtained. Diffusion along the GBs and the junctions is allowed so as to prevent nucleation of voids and overlapping of material near the GBs. The coupled dynamics has been studied in detail for two bicrystalline and one tricrystalline arrangements. The first bicrystal consists of two cubic grains separated by a planar GB, whereas the second is composed of a spherical grain embedded inside a larger grain. The tricrystal has an arbitrary-shaped grain embedded inside a much larger bicrystal made of two cubic grains. In all these cases, analytical solutions are obtained wherever possible while emphasizing the role of various kinetic coefficients during the coupled motion.

1. Introduction

We develop a thermodynamically consistent continuum framework to study three-dimensional coupled grain boundary (GB) motion in the presence of triple junctions. A GB is modelled as a sharp incoherent interface connected to other GBs at junction curves. The irreversible dynamics at a GB is governed by its normal motion (GB migration) and a relative tangential sliding of the adjacent grains. The latter can arise owing to the intergranular viscous sliding, possibly as a result of the twist component of the GB, or/and as a result of coupling with GB migration [1].

THE ROYAL SOCIETY PUBLISHING

In polycrystalline materials with rigidly deforming grains, as will be assumed presently, the sliding can be decomposed into a relative translation and a relative rotation between the adjacent grains. On the other hand, the irreversible dynamics at a junction is governed by the motion of the non-splitting junction curve. The presence of junctions can significantly influence the overall dynamics of all the GBs and the grains in their neighbourhood, for instance by inducing drag or altering diffusive flux [2]. The coupled motion, which requires sliding to be necessarily coupled with GB migration, is the dominant mechanism for both grain coarsening and plastic deformation in nanocrystalline (NC) materials with average grain size of the order of few tens of nanometres (hence a large volume fraction of GBs and triple junctions) [3,4]. This is unlike coarse-grained materials where GB migration and dislocation dynamics dominate grain coarsening and plastic deformation, respectively. The coupled motion has recently been studied theoretically [1,2,5,6], experimentally [7] and with molecular simulations [8]. Although some of these studies have included the effect of junction dynamics [2,8], all of them are restricted to two-dimensional grains and hence applicable only to polycrystals where each grain is columnar and identical in cross section along the length direction; such a restriction requires the GB to have only tilt, and no twist, character.

The main contributions of this paper include:

(1) A three-dimensional thermodynamic formalism including diffusion to deal with incoherent interfaces with junctions (§3). Junctions have been previously studied in the context of continuum thermodynamics but only with coherent interfaces and without diffusion [9,10]. On the other hand, thermodynamics of incoherent interfaces has been explored earlier without considering junctions [11]. All of these works were based on the framework of configurational mechanics. Our treatment, while extending to junctions with incoherent interfaces, takes an alternate viewpoint where we do not regard the configurational forces to be fundamentally on the same footing as standard forces (with their own balance laws, etc.). We introduce configurational forces in our formalism as mechanisms of internal power generation so as to ensure that the excess entropy production is restricted to interfaces and junctions. A two-dimensional version of this formalism was recently presented by the authors [2].
(2) Deriving kinetic relations for coupled GB motion in three dimensions (§4). The phenomenological kinetic equations are motivated from the dissipation inequalities derived from the second law of thermodynamics in confirmation with other standard balance laws of continuum physics. Our results extend earlier models of coupled GB motion to a three-dimensional setting. The first kinetic relations for the coupled motion were proposed by Cahn & Taylor [1,5] which were restricted to two-dimensions and only bicrystalline arrangements (hence no junctions). They also ignored the possibility of relative translation of grains while considering sliding at the GB only owing to the relative rotation. More recently, Basak & Gupta [2] have extended the model to include junctions and relative translation but still restricting themselves to two dimensions.
(3) Formulation of a vectorial geometrical coupling factor (appendix A). The coupling between the tangential and the normal motion of the GB is purely geometric and depends on the measure of incoherency at the boundary [1,12,13]. The incoherency is quantified by the net Burgers vector (given by Frank–Bilby relation) or equivalently by the interfacial dislocation density. The GBs in the present three-dimensional framework generally have a mixed character with both tilt and twist components. The coupling factor for a high angle planar symmetric tilt boundary, derived previously by Cahn *et al.* [12,13], therefore, needs to be extended to include multiple sets of edge and screw dislocation arrays. The coupling factor now derived is a vectorial quantity rather than a scalar as has been the case in the earlier studies.

Our derivations are based on the following assumptions: (i) the individual grains experience only rigid deformations (i.e. translations and rotations); the deformations are, however, allowed

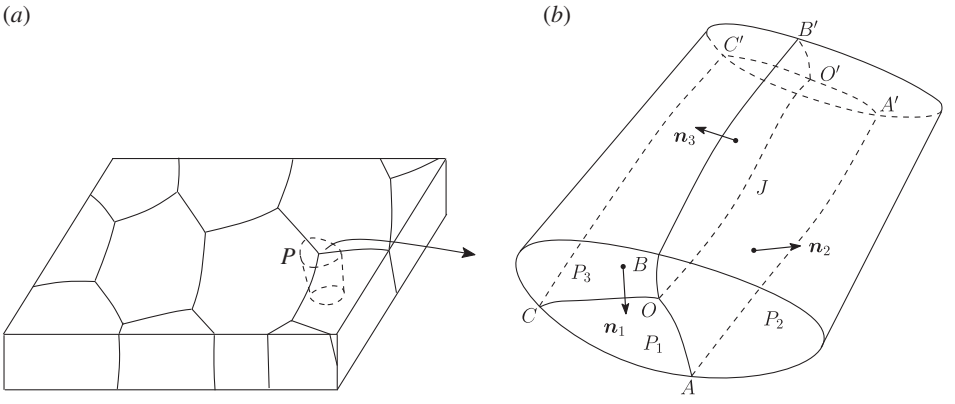

Figure 1. (*a*) Schematic of a polycrystal in three-dimension. (*b*) The region P containing three subregions P_1, P_2 and P_3. The GBs $OO'A'A$, $OO'B'B$ and $OO'C'C$ (with normals $\boldsymbol{n}_1$, $\boldsymbol{n}_2$ and $\boldsymbol{n}_3$, as shown) are denoted by Γ_1, Γ_2 and Γ_3, respectively. The curve OO' is the triple junction J.

to remain finite, (ii) the shape accommodation required for preventing void nucleation and interpenetration of the material in proximity of the GBs, during relative tangential motion between the grains, is accomplished by diffusion across as well as along the GBs and also along the junction curves; (iii) the velocities associated with various GBs, grains and junctions remain much smaller than the speed of sound in the material. The inertial effects are therefore ignored; (iv) the grains are free of defects and all the lattice imperfections are concentrated at the GBs and the junctions (this is reasonable for NC materials with their small grain size); and (v) no additional stress fields are present at the interface and the junction. The GBs are considered to be orientable surfaces (of arbitrary shapes) with five macroscopic degrees of freedom which include three misorientation angles and two independent variables describing the orientation of the GB. The junctions are arbitrary three-dimensional space curves with varying curvature, normal, binormal, torsion, etc. The excess energy density of a GB is assumed to depend on the five parameters (and additionally the curvature) mentioned above, whereas the excess energy density of a junction is assumed to depend only on the unit tangent associated with the junction curve.

The paper is organized in the following manner. In §2, we briefly introduce various geometrical preliminaries, including integral relations, required for our study. We derive the essential balance laws and dissipation inequalities in §3. In §4, we apply our theory to derive the kinetic relations for GB motion, grain dynamics and junction motion for two bicrystalline and one tricrystalline arrangements. A generalized derivation of the vectorial geometrical coupling factor is presented in appendix A. We conclude our study with a discussion on some open directions in §5.

2. Geometrical preliminaries

Let $\mathcal{E}$ be a three-dimensional Euclidean point space whose translational space (set of vectors) is denoted by $\mathcal{V}$. Because we are dealing with finite dimensional Euclidean spaces, we do not distinguish them from their dual. The set of second-order tensors consist of all linear transformations from $\mathcal{V}$ to itself. Consider a region $P \in \mathcal{E}$, as shown in figure 1*b*, taken out from a polycrystalline arrangement depicted in figure 1*a*. It contains three subgrains P_1, P_2 and P_3, three smooth GBs Γ_1, Γ_2 and Γ_3, and a smooth junction curve J. The normal $\boldsymbol{n}_i$ to Γ_i is chosen such that it points inside P_i, where $i = 1, 2, 3$. We denote the position vector of a point in P by $\boldsymbol{x}$ and the time by t. The grains are oriented differently with respect to a fixed coordinate.

Let $\boldsymbol{A}$ and $\boldsymbol{B}$ be second-order tensors. The derivative of a scalar-valued differentiable function of tensors, say $G(\boldsymbol{A})$, is a tensor $\partial_{\boldsymbol{A}} G$ defined by $G(\boldsymbol{A}+\boldsymbol{B}) = G(\boldsymbol{A}) + \partial_{\boldsymbol{A}} G \cdot \boldsymbol{B} + o(|\boldsymbol{B}|)$, where $o(|\boldsymbol{B}|)/|\boldsymbol{B}| \to 0$ as $|\boldsymbol{B}| \to 0$; the norm of a tensor is defined as $|\boldsymbol{B}|^2 = \boldsymbol{B} \cdot \boldsymbol{B}$, where $(\cdot)$

represents the Euclidean inner product. Similar definitions can be made for vector and tensor-valued differentiable functions (of scalars, vectors and tensors). ∇ indicates the gradient of a differentiable field defined over P.

(a) Bulk fields

Let f be a piecewise-smooth bulk field which is discontinuous across Γ_i and singular at J. We denote the jump of f across Γ_i as $[\![f]\!] = f^+ - f^-$, where f^+ is the limiting value of f at $\boldsymbol{x} \in \Gamma_i$ from the grain into which $\boldsymbol{n}_i$ points and f^- is the limiting value from the other grain. If f_1 and f_2 are two piecewise continuous functions across Γ_i, and the product $f_1 f_2$ is distributive with respect to the sum, then $[\![f_1 f_2]\!] = [\![f_1]\!]\langle f_2\rangle + \langle f_1\rangle [\![f_2]\!]$, where $\langle f\rangle = (f^+ + f^-)/2$ is the average of f^+ and f^-. To deal with the singularity of the field at the junction, we carry out our analysis in a punctured region P_ϵ obtained by excluding a small tube T_ϵ of radius ϵ from P in the neighbourhood of the junction, cf. [9]. The outward normal to the boundary of the tube ∂T_ϵ is denoted by $\boldsymbol{m}$. The boundary ∂T_ϵ moves with a velocity $\boldsymbol{u}$.

We assume that f satisfies the limit

$$\int_P f dv = \lim_{\epsilon \to 0} \int_{P_\epsilon} f dv, \tag{2.1}$$

where dv is the volume measure on P. Using the standard transport relations for the bulk quantities, it can be shown that [9]

$$\frac{\mathrm{d}}{\mathrm{d}t} \int_P f dv = \int_P (\dot{f} + f \mathrm{div} \boldsymbol{v}) dv - \sum_{i=1}^{3} \int_{\Gamma_i} [\![f U_i]\!] da - \lim_{\epsilon \to 0} \int_{\partial T_\epsilon} f\, (\boldsymbol{u} - \boldsymbol{v}) \cdot \boldsymbol{m} da, \tag{2.2}$$

where the superposed middle dot denotes the material time derivative, div is the divergence operator, $\boldsymbol{v}$ is the particle velocity, V_i is the interfacial normal velocity, $U_i = V_i - \boldsymbol{v} \cdot \boldsymbol{n}_i$ is the relative normal velocity of the interface and da is the area measure on a surface. Let $\boldsymbol{a}$ and $\boldsymbol{A}$ denote a piecewise-smooth vector and tensor field, respectively, defined in P but allowed to be singular at the junction. The divergence theorem requires [9]

$$\int_P \mathrm{div} \boldsymbol{a} dv = \int_{\partial P} \boldsymbol{a} \cdot \boldsymbol{m} da - \sum_{i=1}^{3} \int_{\Gamma_i} [\![\boldsymbol{a}]\!] \cdot \boldsymbol{n}_i da - \lim_{\epsilon \to 0} \int_{\partial T_\epsilon} \boldsymbol{a} \cdot \boldsymbol{m} da \tag{2.3}$$

and

$$\int_P \mathrm{div} \boldsymbol{A} dv = \int_{\partial P} \boldsymbol{A} \boldsymbol{m} da - \sum_{i=1}^{3} \int_{\Gamma_i} [\![\boldsymbol{A}]\!] \boldsymbol{n}_i da - \lim_{\epsilon \to 0} \int_{\partial T_\epsilon} \boldsymbol{A} \boldsymbol{m} da. \tag{2.4}$$

(b) Interfacial fields

Consider an orientable surface Γ (subscript i is presently dropped), with boundary a closed piecewise-smooth curve $\partial\Gamma$, and let $\boldsymbol{n}$ and V be the associated unit normal field and normal velocity field, respectively. The surface gradient of a scalar field g, vector field $\boldsymbol{g}$ and tensor field $\boldsymbol{G}$, all smoothly defined over Γ, are defined as

$$\nabla^S g = \boldsymbol{P}(\nabla g), \quad \nabla^S \boldsymbol{g} = (\nabla \boldsymbol{g})\boldsymbol{P} \quad \text{and} \quad \nabla^S \boldsymbol{G} = (\nabla \boldsymbol{G})\boldsymbol{P}, \tag{2.5}$$

respectively, where $\boldsymbol{P} = \boldsymbol{I} - \boldsymbol{n} \otimes \boldsymbol{n}$ is the projection tensor ($\boldsymbol{I}$ is the identity tensor and $\otimes$ denotes the dyadic product); while calculating ∇g (etc.), one has to use a smooth extension of g in a small neighbourhood of Γ. The surface divergence of these fields is defined by

$$\mathrm{div}^S \boldsymbol{g} = \mathrm{tr}(\nabla^S \boldsymbol{g}) \quad \text{and} \quad \boldsymbol{k} \cdot \mathrm{div}^S \boldsymbol{G} = \mathrm{div}^S (\boldsymbol{G}^{\mathrm{T}} \boldsymbol{k}), \tag{2.6}$$

for all constant vectors $\boldsymbol{k}$, where tr represents the trace operator and the superscript 'T' stands for the transpose. The surface Laplacian of g is given by $\Delta^S g = \mathrm{div}^S (\nabla^S g)$. The curvature tensor field $\boldsymbol{L}$ and the total curvature κ associated with Γ are defined as $\boldsymbol{L} = -\nabla^S \boldsymbol{n}$ and $\kappa = \mathrm{tr} \boldsymbol{L}$, respectively.

Let $\boldsymbol{t}$ be the outward unit normal to the closed curve $\partial\Gamma$ such that $\boldsymbol{n}\cdot\boldsymbol{t}=0$. When $\boldsymbol{G}$ and $\boldsymbol{g}$ satisfy $\boldsymbol{G}\boldsymbol{n}=\boldsymbol{0}$ and $\boldsymbol{g}\cdot\boldsymbol{n}=0$, respectively, the surface divergence theorem yields [14]

$$\int_{\partial\Gamma}\boldsymbol{G}\boldsymbol{t}dl=\int_{\Gamma}\mathrm{div}^S\boldsymbol{G}da\quad\text{and}\quad\int_{\partial\Gamma}\boldsymbol{g}\cdot\boldsymbol{t}dl=\int_{\Gamma}\mathrm{div}^S\boldsymbol{g}da, \tag{2.7}$$

where dl is the length measure of a curve.

The normal time derivative of g following Γ is given by $\overset{\circ}{g}=\dot{g}+V\nabla g\cdot\boldsymbol{n}$, which represents the rate of change of g as experienced by an observer sitting on the moving surface Γ [14]. The first term indicates the local rate of change of g at a fixed material position, whereas the second term represents the rate of change of g owing to influx of particles along $\boldsymbol{n}$ as the interface moves with velocity V. The following identities can be readily verified [15]:

$$\overset{\circ}{\boldsymbol{n}}=-\nabla^S V\quad\text{and}\quad\overset{\circ}{\boldsymbol{L}}=-\nabla^S\overset{\circ}{\boldsymbol{n}}-\boldsymbol{L}\overset{\circ}{\boldsymbol{n}}\otimes\boldsymbol{n}+V\boldsymbol{L}^2. \tag{2.8}$$

On the other hand, the intrinsic time derivative of g following $\partial\Gamma$ is given by $\overset{\square}{g}=\dot{g}+\nabla g\cdot\boldsymbol{w}$, where $\boldsymbol{w}$ is the intrinsic velocity of $\partial\Gamma$, such that $\boldsymbol{w}=V\boldsymbol{n}+W\boldsymbol{t}$, and W is the velocity of $\partial\Gamma$ along $\boldsymbol{t}$ [15]. Thus, $\overset{\square}{g}$ is equal to the sum of the rate of change of g following Γ and a term representing the change in g owing to the incoming particles from the neighbourhood along the tangential direction $\boldsymbol{t}$.

We will need the following transport theorem for Γ such that a part of $\partial\Gamma$ intersects with ∂P and the rest with J [9]:

$$\frac{\mathrm{d}}{\mathrm{d}t}\int_{\Gamma}gda=\int_{\Gamma}(\overset{\circ}{g}-g\kappa V)da+\int_{\Gamma\cap\partial P}gWdl+\int_{J}g\boldsymbol{q}_p\cdot\boldsymbol{t}dl, \tag{2.9}$$

where $\boldsymbol{q}_p$ is the intrinsic (independent of the parametrization) velocity of the junction.

(c) Junction fields

Let δ and ι denote the terminal points of the junction curve J, and let $\boldsymbol{l}$ be the unit tangent to the curve such that it is directed towards ι. The normal and binormal vectors associated with J are denoted by $\boldsymbol{\nu}$ and $\boldsymbol{b}$, respectively. The projection tensor $\boldsymbol{Q}=\boldsymbol{I}-\boldsymbol{\nu}\otimes\boldsymbol{\nu}-\boldsymbol{b}\otimes\boldsymbol{b}=\boldsymbol{l}\otimes\boldsymbol{l}$ maps any vector on to the tangential direction of J. The intrinsic velocity field of the junction, which can be decomposed as $\boldsymbol{q}_p=q_\nu\boldsymbol{\nu}+q_b\boldsymbol{b}$, is such that $(\boldsymbol{I}-\boldsymbol{Q})\boldsymbol{u}\to\boldsymbol{q}_p$ as $\epsilon\to0$ [9]. The velocity of terminal points is denoted as $\hat{\boldsymbol{q}}$ such that $\hat{\boldsymbol{q}}=\boldsymbol{q}_p+\hat{q}_l\boldsymbol{l}$ at the respective endpoints. The intrinsic time derivative of a scalar field defined on the junction curve, say χ, is given by $\overset{\star}{\chi}=\dot{\chi}+\nabla\chi\cdot\boldsymbol{q}_p$. The transport theorem associated with χ is given by [9]

$$\frac{\mathrm{d}}{\mathrm{d}t}\int_{J}\chi dl=\int_{J}(\overset{\star}{\chi}-\chi\kappa_J q_\nu)dl+(\chi\hat{q}_l)_{\delta}^{\iota}, \tag{2.10}$$

where κ_J is the scalar curvature of the junction curve. The gradient of χ along the junction curve is defined as $\nabla^J\chi=\boldsymbol{Q}\nabla\chi$. Similarly, for a vector field defined on J, we introduce $\nabla^J\boldsymbol{q}_p=(\nabla\boldsymbol{q}_p)\boldsymbol{Q}$. We note the identity $\overset{\star}{\boldsymbol{l}}=(\nabla^J\boldsymbol{q}_p)\boldsymbol{l}+q_\nu\kappa_J\boldsymbol{l}$ [9].

It is useful to decompose an integral over the tube surface around the junction as [9]

$$\lim_{\epsilon\to0}\int_{\partial T_\epsilon}\boldsymbol{a}da=\int_{J}\left[\lim_{\epsilon\to0}\oint_{C_\epsilon}\boldsymbol{a}dl\right]dl, \tag{2.11}$$

where ∂T_ϵ is the envelope of the circles C_ϵ of radius ϵ.

3. Balance laws and dissipation

We now obtain the consequences of balance of mass and momentum, as well as obtain local dissipation inequalities in the bulk, at the interface, and at the junction, while restricting to

the assumptions enlisted in §1. In particular, we allow the individual grains to deform only rigidly, although without restricting the magnitude of the deformation so as to accommodate large intergranular slip and grain rotation.

(a) Balance of mass

The rate of change of total mass in P is balanced by the mass transport into the region via bulk diffusion across ∂P, GB diffusion at the edge $\Gamma_i \cap \partial P$, and diffusion at ι and δ. Neglecting excess mass densities of the GBs and the junction, the mass balance can be written as

$$\frac{\mathrm{d}}{\mathrm{d}t}\int_P \rho dv = -\int_{\partial P} \boldsymbol{j}\cdot\boldsymbol{m} da - \sum_{i=1}^{3}\int_{\Gamma_i\cap\partial P} \boldsymbol{h}_i\cdot\boldsymbol{t}_i dl - (h_J)^{\iota}_{\delta}, \tag{3.1}$$

where ρ is the mass density of the bulk grain, $\boldsymbol{j}$ is the bulk diffusional flux, $\boldsymbol{h}_i$ is the tangential diffusional flux on Γ_i, and h_J is the diffusional flux along the junction. Using transport theorem (2.2) and divergence theorems (2.3) and $(2.7)_2$, and localizing the result owing to the arbitrariness of P, we can obtain the following local equations

$$\dot{\rho} + \rho \mathrm{div}\boldsymbol{v} + \mathrm{div}\boldsymbol{j} = 0 \quad \forall \boldsymbol{x} \in P_i, \tag{3.2}$$

$$[\![\rho U_i]\!] = [\![\boldsymbol{j}]\!]\cdot\boldsymbol{n}_i + \mathrm{div}^S \boldsymbol{h}_i \quad \forall \boldsymbol{x} \in \Gamma_i \tag{3.3}$$

and

$$\lim_{\epsilon\to 0}\oint_{C_\epsilon} \rho(\boldsymbol{u}-\boldsymbol{v})\cdot\boldsymbol{m} dl = \nabla^J h_J\cdot\boldsymbol{l} + \lim_{\epsilon\to 0}\oint_{C_\epsilon} \boldsymbol{j}\cdot\boldsymbol{m} dl - \sum_{i=1}^{3}(\boldsymbol{h}_i\cdot\boldsymbol{t}_i)_J \quad \forall \boldsymbol{x}\in J, \tag{3.4}$$

where we have used the limit $\lim_{\epsilon\to 0}\sum_{i=1}^{3}\int_{\partial T_\epsilon\cap\Gamma_i}\boldsymbol{h}_i\cdot\boldsymbol{t}_i dl = \sum_{i=1}^{3}\int_J(\boldsymbol{h}_i\cdot\boldsymbol{t}_i)_J dl$.

Here, and in rest of this paper, we have considered contact interactions to be concentrated over edges and points. These are to be understood in terms of the physical concentration of the relevant quantity over the respective domain. In contrast, if these interactions were to take place at edges and points which represent geometrical singularities on the boundary of P, then we would require a higher gradient theory to justify their existence [16].

(b) Balance of linear momentum

Neglecting inertia and body forces, and assuming absence of interfacial and junction stress fields, the balance of linear momentum is given by

$$\int_{\partial P} \boldsymbol{\sigma}\boldsymbol{m} da = \boldsymbol{0}, \tag{3.5}$$

where $\boldsymbol{\sigma}$ is the symmetric Cauchy stress tensor. Using (2.4), the following local equations are readily obtained [9]

$$\mathrm{div}\boldsymbol{\sigma} = \boldsymbol{0} \quad \forall \boldsymbol{x}\in P_i, \tag{3.6}$$

$$[\![\boldsymbol{\sigma}]\!]\boldsymbol{n}_i = \boldsymbol{0} \quad \forall \boldsymbol{x}\in\Gamma_i \tag{3.7}$$

and

$$\lim_{\epsilon\to 0}\oint_{C_\epsilon}\boldsymbol{\sigma}\boldsymbol{m} dl = \boldsymbol{0} \quad \forall \boldsymbol{x}\in J. \tag{3.8}$$

According to (3.7), the traction field is continuous across the GBs, whereas (3.8) requires that the net force acting at each circular region C_ϵ is zero in the limit $\epsilon\to 0$, although the stress field can still be singular at the junction (weak singularity).

(c) Dissipation inequality

Let Ψ be the bulk free energy density, γ_i the interfacial free energy per unit area of Γ_i, and η the free energy per unit length of J. For an isothermal environment, the mechanical version of the second law requires the rate of change of the total free energy pertaining to P to be less than or equal to the total power input into P [14,17], i.e.

$$\frac{\mathrm{d}}{\mathrm{d}t}\left(\int_P \Psi\, dv + \sum_{i=1}^{3}\int_{\Gamma_i}\gamma_i da + \int_J \eta dl\right) \leq \int_{\partial P} \boldsymbol{\sigma}\boldsymbol{m}\cdot\boldsymbol{v} da - \int_{\partial P}\mu \boldsymbol{j}\cdot\boldsymbol{m} da - \sum_{i=1}^{3}\int_{\partial P\cap\Gamma_i}\mu \boldsymbol{h}_i\cdot\boldsymbol{t}_i dl - (\mu h_J)_\delta^\iota + \sum_{i=1}^{3}\int_{\partial P\cap\Gamma_i}(\boldsymbol{c}_i\cdot\boldsymbol{w}_i + \boldsymbol{\tau}_i\cdot\overset{\square}{\boldsymbol{n}}_i)dl + (\boldsymbol{\omega}\cdot\hat{\boldsymbol{q}})_\delta^\iota, \tag{3.9}$$

where μ is the chemical potential. We assume that the chemical potential is continuous across the interface and at the junction (i.e. local chemical equilibrium [17]). The first integral on the right-hand side of (3.9) is the power input through the tractions acting on ∂P; the next three terms are contribution to power input owing to mass flux at ∂P, $\partial P\cap\Gamma_i$, and the endpoints of J, respectively. The last two terms are non-standard, and the significance of their appearance in the dissipation inequality needs to be discussed in detail. It is clear that as interfaces evolve, their domain of intersection with P changes; there would be portions of the interface which, previously present outside P, are now inside it, and vice versa. In other words, the set of points belonging to an interface and lying within P changes continuously as the interface evolves. The change in the configuration of interfaces and junction curve within P produces additional entropy at the edges $\partial P\cap\Gamma_i$ and at the terminal points of J. However, in the spirit of Gibbs thermodynamics, we require the excess entropy generation to be necessarily restricted to the GBs and the junction. The non-standard terms are therefore included in the inequality to ensure that there is no excess entropy production at the arbitrary edges and terminal points. These additional power input terms are to be considered in (3.9) only when the edges and the terminal points lie on the surface of an interior part of a body. The precise form of $\boldsymbol{c}_i$, $\boldsymbol{\tau}_i$ and $\boldsymbol{\omega}$ will depend on the constitutive prescriptions for free energies and stress, as well on the nature of allowable dissipative fluxes. At this point, these are to be understood as agents of power input, in conjugation with the respective intrinsic velocities, so as to ensure that the net entropy generation meets the above-mentioned requirement. Such terms also appear in the framework of configurational mechanics [9,11,15], where the existence of $\boldsymbol{c}_i$, $\boldsymbol{\tau}_i$ and $\boldsymbol{\omega}$ is assumed *a priori* as fundamental forces which satisfy certain balance relations. Our treatment (see also [2,6,14]) is motivated purely from the viewpoint of quantifying excess entropy generation. We note that it may be possible to derive the balance laws as well as the global dissipation inequality starting with a more general framework, where the two-dimensional interface is obtained as a limit of a three-dimensional non-material domain, as is done in [18,19]. In doing so, it might be possible to have a better understanding of the non-standard power terms included in (3.9).

Before deriving the consequence of the global dissipation inequality, we briefly digress to discuss the status of configurational balance laws within our framework. In a purely conservative setting (e.g. nonlinear elasticity), these balance laws, which are independent of the standard balance laws, are derived from the horizontal variation of the energy functional [20]. In non-conservative setting such balances are usually postulated (rather than derived) as independent relations [21,22]; an exception is the recent work by Mariano [23,24] where the balance of configurational forces is derived from the invariance of the so-called relative power under roto-translating changes in observers. In our work (see also [2,6]), the configurational balance laws appear in the form of kinetic relations (see §4) which are motivated from the local dissipation inequalities obtained from (3.9). Under equilibrium, they reduce down to the familiar balance laws obtained using variational arguments; for instance, junction kinetic equation reduces to Herring's relation under equilibrium solution (see the end of this subsection). In the

present formalism, non-trivial balances of configurational forces appear only at the interfaces and junctions.

Using transport theorems (2.2), (2.9) and (2.10), divergence theorems (2.3) and (2.7), and the decomposition (2.11), we can rewrite the inequality (3.9) as

$$\sum_{a=1}^{6} I_a \leq 0, \tag{3.10}$$

where

$$I_1 = \int_P (\dot{\Omega} + \Omega \operatorname{div} \boldsymbol{v} + \rho\dot{\mu} - \boldsymbol{\sigma} \cdot \nabla \boldsymbol{v} + \boldsymbol{j} \cdot \nabla\mu) dv, \tag{3.11}$$

$$I_2 = \sum_{i=1}^{3} \int_{P\cap\Gamma_i} (\overset{\circ}{\gamma}_i - \gamma_i \kappa_i V_i - [\![U_i \boldsymbol{E}]\!]\boldsymbol{n}_i \cdot \boldsymbol{n}_i - \langle \boldsymbol{\sigma}\boldsymbol{n}_i \rangle \cdot \boldsymbol{P}_i [\![\boldsymbol{v}]\!] + \boldsymbol{h}_i \cdot \nabla^S \mu) da, \tag{3.12}$$

$$I_3 = \sum_{i=1}^{3} \int_{\partial P\cap\Gamma_i} (\gamma_i W_i - \boldsymbol{c}_i \cdot \boldsymbol{w}_i - \boldsymbol{\tau}_i \cdot \overset{\square}{\boldsymbol{n}}_i) dl, \tag{3.13}$$

$$I_4 = -\int_J \left(\lim_{\epsilon\to 0} \oint_{C_\epsilon} (\boldsymbol{\sigma}\boldsymbol{v} + \Psi(\boldsymbol{u} - \boldsymbol{v}) - \mu\boldsymbol{j}) \cdot \boldsymbol{m} dl \right) dl, \tag{3.14}$$

$$I_5 = \int_J \left(\overset{\star}{\eta} - \eta\kappa_J q_\nu + \nabla^J(\mu h_J) \cdot \boldsymbol{l} + \sum_{i=1}^{3} (\mu \boldsymbol{h}_i \cdot \boldsymbol{t}_i + \gamma_i \boldsymbol{q} \cdot \boldsymbol{t}_i) \right) dl \tag{3.15}$$

and

$$I_6 = (\eta \hat{q}_l - \boldsymbol{\omega} \cdot \hat{\boldsymbol{q}})_\delta^\iota. \tag{3.16}$$

In obtaining (3.11), we have used (3.2) and (3.6), and introduced $\Omega = \Psi - \rho\mu$ (the grand canonical potential). To derive (3.12), on the other hand, we have used (3.3) and (3.7); here, $\boldsymbol{E} = \Omega\boldsymbol{I} - \boldsymbol{\sigma}$ is the projection of the bulk Eshelby tensor on the current configuration.

To determine the precise form of $\boldsymbol{c}_i$, $\boldsymbol{\tau}_i$ and $\boldsymbol{\omega}$, and also to obtain the local dissipation inequalities associated with the grains, GBs and junction, we will now prescribe the constitutive nature of the GB energy and the junction energy. Towards this end, we assume the GB energy to depend on the misorientation between the grains, the normal to the GB and curvature. The former two dependencies are standard in material science literature (cf. ch. 12 in [25]). The curvature dependence is primarily introduced to regularize the governing partial differential equations for capillary-driven GB motion, which otherwise become backward parabolic and hence unstable in certain ranges (GB spinodals) of the orientations. We follow Gurtin & Jabbour [15] in assuming the following quadratic dependence of GB energy on curvature:

$$\gamma = \hat{\gamma}(\boldsymbol{\Theta}, \boldsymbol{n}) + \tfrac{1}{2}\epsilon_1 |\boldsymbol{L}|^2 + \tfrac{1}{2}\epsilon_2 \kappa^2, \tag{3.17}$$

where $\boldsymbol{\Theta}$ is the misorientation tensor given by $(\boldsymbol{R}^+)^{\mathrm{T}}\boldsymbol{R}^-$; ϵ_1 and ϵ_2 are scalar constants such that $\epsilon_1 > 0$ and $\epsilon_2 + \epsilon_1/2 > 0$. The rotation $\boldsymbol{R}^+$ is the orientation tensor of the grain into which $\boldsymbol{n}$ points, and $\boldsymbol{R}^-$ is the orientation tensor of the other grain. We introduce $\boldsymbol{M} \doteq \partial_{\boldsymbol{L}}\gamma = \epsilon_1\boldsymbol{L} + \epsilon_2\kappa\boldsymbol{P}$. It is easy to see that $\boldsymbol{M}$ is symmetric and satisfies $\boldsymbol{M}\boldsymbol{P} = \boldsymbol{M}$. The junction energy density, on the other hand, is assumed to be a function of the unit tangent along the junction curve, i.e. $\eta = \hat{\eta}(\boldsymbol{l})$ [9]. Substituting these into (3.10), and performing a cumbersome but straightforward calculation, yields

$$\begin{aligned} &\int_P \mathfrak{D}_b dv + \sum_{i=1}^{3} \int_{\Gamma_i} \mathfrak{D}_{\Gamma_i} da + \int_J \mathfrak{D}_J dl - \sum_{i=1}^{3} \int_{\partial P\cap\Gamma_i} \{W_i(\gamma_i - \boldsymbol{M}_i\boldsymbol{L}_i\boldsymbol{t}_i \cdot \boldsymbol{t}_i - \boldsymbol{c}_i \cdot \boldsymbol{t}_i) \\ &\quad - V_i((\operatorname{div}^S \boldsymbol{M}_i + \partial_{\boldsymbol{n}_i}\hat{\gamma}_i) \cdot \boldsymbol{t}_i + \boldsymbol{c}_i \cdot \boldsymbol{n}_i) - \overset{\square}{\boldsymbol{n}}_i \cdot (\boldsymbol{\tau}_i + \boldsymbol{M}_i\boldsymbol{t}_i)\} dl \\ &\quad - (\hat{q}_l(\eta - \omega_l) + ((\boldsymbol{I} - \boldsymbol{Q})\partial_l\hat{\eta} - \boldsymbol{\omega}_p) \cdot \boldsymbol{q}_p)_\delta^\iota \geq 0, \end{aligned} \tag{3.18}$$

where $\mathfrak{D}_b$, $\mathfrak{D}_{\Gamma_i}$ and $\mathfrak{D}_J$ are the entropy generation rates per unit volume of the bulk, per unit area of Γ_i, and per unit length of J, respectively. The expressions for these rates are given in equations (3.21)–(3.23). In deriving the above inequality, we have also assumed the junctions to be non-splitting, i.e. $V_i = \boldsymbol{q}_p \cdot \boldsymbol{n}_i$. The first term in the above inequality is the net entropy generation within the grains. The next two terms are excess entropy generation at the GBs and at the junction, respectively. The rest of terms in (3.18) are the entropy production rate at the edges $\Gamma_i \cap \partial P$, and the terminal points δ and ι. We however require that the excess entropy production must not have any contribution from the edges of the GBs and the terminal points of J, all of which are a part of ∂P. This is reasonable, because the entropy generation in P should only be within the grains, at the interfaces, and at the junction. Any additional source should vanish. Consequently,

$$\boldsymbol{c}_i \cdot \boldsymbol{t}_i = \gamma_i - \boldsymbol{M}_i \boldsymbol{L}_i \boldsymbol{t}_i \cdot \boldsymbol{t}_i, \quad \boldsymbol{c}_i \cdot \boldsymbol{n}_i = -\left(\mathrm{div}^S \boldsymbol{M}_i + \partial_{\boldsymbol{n}_i} \hat{\gamma}_i\right) \cdot \boldsymbol{t}_i, \tag{3.19}$$

$$\boldsymbol{\tau}_i = -\boldsymbol{M}_i \boldsymbol{t}_i, \quad \text{and} \quad \boldsymbol{\omega} = \eta \boldsymbol{l} + (\boldsymbol{I} - \boldsymbol{Q}) \partial_{\boldsymbol{l}} \hat{\eta}. \tag{3.20}$$

Substituting (3.19) and (3.20) back into (3.18), and localizing the result, we obtain the following local dissipation inequalities

$$\mathfrak{D}_b = \boldsymbol{\sigma} \cdot \nabla \boldsymbol{v} - (\dot{\Omega} + \Omega \mathrm{div} \boldsymbol{v}) - \rho \dot{\mu} - \boldsymbol{j} \cdot \nabla \mu \geq 0 \quad \forall \boldsymbol{x} \in P_i, \tag{3.21}$$

$$\mathfrak{D}_{\Gamma_i} = [\![U_i \boldsymbol{E}]\!] \boldsymbol{n}_i \cdot \boldsymbol{n}_i + \langle \boldsymbol{\sigma} \boldsymbol{n}_i \rangle \cdot \boldsymbol{P}_i [\![\boldsymbol{v}]\!] - \boldsymbol{h}_i \cdot \nabla^S \mu + f_i V_i - (\partial_{\boldsymbol{\Theta}_i} \hat{\gamma}_i) \cdot \dot{\boldsymbol{\Theta}}_i \geq 0 \quad \forall \boldsymbol{x} \in \Gamma_i \tag{3.22}$$

and

$$\mathfrak{D}_J = \boldsymbol{\mathcal{F}}_J \cdot \boldsymbol{q}_p - \lim_{\epsilon \to 0} \oint_{C_\epsilon} \boldsymbol{E} \boldsymbol{m} \cdot \boldsymbol{v} dl - h_J (\nabla^J \mu) \cdot \boldsymbol{l} - \sum_{i=1}^{3} \boldsymbol{\tau}_i \cdot \boldsymbol{n}_i^\star \geq 0 \quad \forall \boldsymbol{x} \in J, \tag{3.23}$$

where

$$f_i = \gamma_i \kappa_i - \mathrm{div}^S (\partial_{\boldsymbol{n}_i} \hat{\gamma}_i) - \boldsymbol{M}_i \cdot \boldsymbol{L}_i^2 - \mathrm{div}^S (\mathrm{div}^S \boldsymbol{M}_i), \tag{3.24}$$

$$\boldsymbol{\mathcal{F}}_J = (\boldsymbol{I} - \boldsymbol{Q}) \left(\lim_{\epsilon \to 0} \oint_{C_\epsilon} \boldsymbol{E} \boldsymbol{m} dl - \sum_{i=1}^{3} \boldsymbol{c}_i - f_J \right) \tag{3.25}$$

and

$$\boldsymbol{f}_J = -\eta \kappa_J \boldsymbol{v} + \nabla^J ((\boldsymbol{I} - \boldsymbol{Q}) \partial_{\boldsymbol{l}} \hat{\eta}) \boldsymbol{l}. \tag{3.26}$$

Equation (3.21) gives the entropy production rate per unit volume within the grain. For rigidly deforming grains $\boldsymbol{\sigma} \cdot \nabla \boldsymbol{v} = 0$ and $\mathrm{div} \boldsymbol{v} = 0$. Additionally, if we assume that $\Psi = \hat{\Psi}(\rho)$, then (3.21) yields $\mu = \partial_\rho \hat{\Psi}$ and $\boldsymbol{j} \cdot \nabla \mu \leq 0$. Equation (3.22) contains the dissipation rate per unit area of the GB, with contribution from boundary migration, relative translation of grains at the boundary, GB diffusion and misorientation change. The inequality therein forms a basis for postulating kinetic relations for coupled GB motion, as is done in §4. It can also be a starting point for motivating kinetic relations for motion of incoherent phase boundaries with diffusion- and curvature-dependent boundary energy [11,15], as well as for a variety of physical phenomena involving coherent interfaces [17]. An analogous inequality, valid for a one-dimensional interface in a two-dimensional grain, was derived recently by Basak & Gupta [6].

Equation (3.23) gives the net dissipation rate per unit length of the junction curve, with contribution owing to motion of the curve, diffusion along it, and evolution of orientation of the intersecting boundaries. A comment is in order regarding the contribution owing to the latter, represented by the last term on the LHS of the inequality. It is evident that this term is linear in scalar parameters (ϵ_1 and ϵ_2) which appear in the curvature-dependent part of the GB energy. The scalar parameters are usually infinitesimally small, ensuring that curvature-dependent part of the energy is significant only at the corners [15]. The curvatures of intersecting boundaries, as they approach the junction, are finite and hence $|\boldsymbol{\tau}_i|$ are small. We can therefore ignore the last term on the LHS of the inequality (3.23) within the present analysis. Second, in the context of GB dynamics, we assume the density field to remain bounded at the junction curve and the velocity

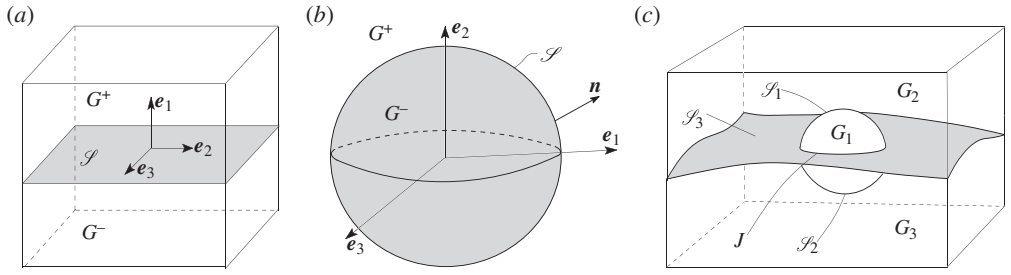

Figure 2. (*a*) Schematic of bicrystal-I. (*b*) Schematic of bicrystal-II. (*c*) Schematic of tricrystal.

in each grain to be resulting only a simple rigid body motion (hence no strains in the grain). With these assumptions, and keeping in mind the weak singularity condition (3.8), we can show that the closed integral terms in (3.23) vanish in the limiting sense. We can rewrite (3.23) and (3.25) under all these considerations as

$$\mathfrak{D}_J = \boldsymbol{\mathcal{F}}_J \cdot \boldsymbol{q}_p - h_J(\nabla^J \mu) \cdot \boldsymbol{l} \geq 0 \quad \forall\, \boldsymbol{x} \in J, \quad \text{where} \tag{3.27}$$

$$\boldsymbol{\mathcal{F}}_J = -(\boldsymbol{I} - \boldsymbol{Q}) \left(\sum_{i=1}^{3} \boldsymbol{c}_i + \boldsymbol{f}_J \right). \tag{3.28}$$

During thermodynamic equilibrium, with junction curve remaining stationary and diffusion absent, $\boldsymbol{\mathcal{F}}_J = \boldsymbol{0}$ which in the absence of junction energy yields the well-known Herring's relation [26], i.e. $\sum_{i=1}^{3}(\gamma_i \boldsymbol{t}_i - \partial_{\boldsymbol{n}_i}\gamma_i) = \boldsymbol{0}$. The above framework can be used to obtain the extension of Herring's relation in the presence of junction energy and various singular fields (see also [9]). Finally, we note that junctions have been previously treated in the framework of continuum thermodynamics but only for intersecting boundaries which are coherent [9,10]. The grain boundaries, however, are in general incoherent and a treatment of coupled GB motion necessarily requires allowance for relative slip at the boundary. The present framework allows for such incoherency and for junctions which are formed at the intersection of such boundaries.

4. Kinetic relations

The governing equations for coupled GB dynamics with junctions can be derived starting from inequalities (3.22) and (3.23) by first identifying various dissipative fluxes, and the associated driving forces and then assuming linear kinetics. Towards this end, we can use Onsager's relations [27] in an unambiguous manner, because fluxes are clearly defined as time-rate of change of the state variables. That this is not so in general, as in the case of heat conduction and viscous flow, has been pointed out by Truesdell [28]. We illustrate the derivation of kinetic relations using three crystalline arrangements as described in the following subsections.

(a) Bicrystal-I

The first bicrystalline arrangement is as shown in figure 2*a* such that the traction on the outer boundaries perpendicular to $\boldsymbol{e}_1$ is $\tau \boldsymbol{e}_2$ and the traction on the outer boundaries perpendicular to $\boldsymbol{e}_2$ is $\tau \boldsymbol{e}_1$. We neglect all kinds of atomic diffusion. The GB $\mathcal{S}$ is considered to be of a mixed type, with both tilt and twist components, where the misorientation is given by $\boldsymbol{\Theta} = \boldsymbol{I} + \theta_1(\boldsymbol{e}_1\times) + \theta_3(\boldsymbol{e}_3\times)$ for small θ_1 and θ_3, where $(\boldsymbol{e}\times)$ represents a skew tensor with components given by $(\boldsymbol{e}\times)_{jk} = \varepsilon_{jlk}e_l$ (here ε_{jlk} is the permutation symbol); as discussed in appendix A, θ_1 and θ_3 determine the twist and the tilt characteristic, respectively, of the GB. Whereas the deformation of grains in the wake of a moving GB, under the external loading considered here, is simple shear for a tilt GB, it is more complicated if the GB is of mixed type [7]. The array of edge dislocations is driven by the

Peach–Koehler force to move the GB in normal direction while translating the grains parallel to the GB. On the other hand, the simultaneous movement of two perpendicular sets of screw dislocation arrays results into a relative rotation of the adjacent grains about the GB normal. The GB motion, the relative tangential translation and the grain rotation are, in general, all coupled to each other.

The state of stress throughout the bicrystal is taken as $\boldsymbol{\sigma} = \tau(\boldsymbol{e}_2 \otimes \boldsymbol{e}_1 + \boldsymbol{e}_1 \otimes \boldsymbol{e}_2)$; this clearly satisfies both the equilibrium equations and the traction boundary conditions. Based on the experimental observations in [7,29], we assume the tilt angle to remain fixed while allowing the twist angle to evolve owing to the relative rotation between the grains. The axis of rotation is taken to coincide with $\boldsymbol{e}_1$. Without loss of generality, the grain G^+ can be assumed to remain stationary, i.e. $\boldsymbol{v}^+ = \boldsymbol{0}$, and G^- moving with a velocity $\boldsymbol{v}^- = \dot{\theta}_1 \boldsymbol{e}_1 \times \boldsymbol{x} + \dot{C}\boldsymbol{e}_2$, where $\dot{C}$ is the translational velocity of G^- in the direction of $\boldsymbol{e}_2$ and $\boldsymbol{x} = x_1\boldsymbol{e}_1 + x_2\boldsymbol{e}_2 + x_3\boldsymbol{e}_3$ is the position vector. Observing that $[\![v_n]\!] = 0$, the dissipation inequality (3.22) reduces to $\dot{\theta}_1 f_\theta + \dot{C} f_c \geq 0$, $\forall\, \boldsymbol{x} \in \mathcal{S}$, where $f_\theta = (\tau x_3 - \partial\gamma/\partial\theta_1)$ and $f_c = -\tau$. Following Onsager, we postulate the following pair of coupled kinetic relations [6]:

$$\dot{\theta}_1 = \mathcal{S}_d f_\theta + \mathcal{B}\mathcal{S}_d f_c \quad \text{and} \quad \dot{C} = \mathcal{B}\dot{\theta}_1 + \mathcal{L} f_c, \tag{4.1}$$

where $\mathcal{S}_d \geq 0$ is the sliding coefficient owing to the relative rotational motion (caused by the intrinsic screw dislocation glide along $\mathcal{S}$), $\mathcal{L} \geq 0$ is the sliding coefficient for the relative translational motion between the grains and $\mathcal{B}$ denotes a coupling between grain rotation and translation. In response to grain translation, the edge dislocation array will cause simultaneous GB migration [12], such that $V = -\dot{C}/\beta_2$, where $\beta_2 = \theta_3$ is the geometrical coupling factor as calculated in the previous section. Note that the geometrical coupling exists only with respect to the translational velocity, as the rotational part of $\boldsymbol{v}^-$ amount to pure sliding. Accordingly, it is the direction of $\dot{C}$ which decides whether the GB will move upwards or downwards. We have a coupled system of equations which should be solved to evaluate the position of the grains and the GB, as well as the misorientation, at any given time instance during the dynamical process. It should be noted that, in a more complicated situation when the driving forces are functions of x_1 and x_2, an initially planar GB will not necessarily remain planar (cf. [7]) and GB diffusion will be required to prevent void-formation/interpenetration at the GB.

(b) Bicrystal-II

We consider a bicrystal with a spherical grain G^- (of radius R) embedded within a much larger grain G^+, as shown in figure 2*b*, with misorientation between the grains given by $\boldsymbol{\Theta} = \boldsymbol{I} + \theta_1(\boldsymbol{e}_1\times) + \theta_2(\boldsymbol{e}_2\times) + \theta_3(\boldsymbol{e}_3\times)$; i.e. grain G^- was obtained by rotating it from G^+ by small angles θ_1, θ_2 and θ_3 about $\boldsymbol{e}_1$, $\boldsymbol{e}_2$ and $\boldsymbol{e}_3$, respectively, where the orthonormal basis vectors $\{\boldsymbol{e}_1, \boldsymbol{e}_2, \boldsymbol{e}_3\}$ form a coordinate frame with origin at the centre of the sphere. The GB $\mathcal{S}$ hence is of a mixed type. Without loss of generality, we let the outer grain G^+ to remain fixed and allow the inner grain G^- to rotate (without translating). We assume that the external stress is absent, the grains are rigid and free of defects, the free energy of the grains is vanishing, and the volumetric diffusion is absent. Let us consider an orthonormal spherical basis $\{\boldsymbol{e}_R, \boldsymbol{e}_\xi, \boldsymbol{e}_\phi\}$ with origin at the centre of the embedded grain (ξ is the polar angle and ϕ is the azimuthal angle). The GB normal $\boldsymbol{n}$ points into G^+, hence $\boldsymbol{n} = \boldsymbol{e}_R$. The angular velocity of G^- (axial vector of $\dot{\boldsymbol{\Theta}}$) is given by $\boldsymbol{w} = \dot{\theta}_1\boldsymbol{e}_1 + \dot{\theta}_2\boldsymbol{e}_2 + \dot{\theta}_3\boldsymbol{e}_3$. Neglecting rigid body translation, the velocity of the inner grain can be written as $\boldsymbol{v}^- = \boldsymbol{w} \times \boldsymbol{x}$, where $\boldsymbol{x}$ is the position vector. Recalling that $\boldsymbol{v}^+ = \boldsymbol{0}$ we obtain $[\![v_n]\!] = v_n^+ = 0$ and $\boldsymbol{V}_\mathrm{t} = \boldsymbol{P}(\boldsymbol{v}^+ - \boldsymbol{v}^-) = -\boldsymbol{v}^-$, where $\boldsymbol{V}_\mathrm{t}$ represents the relative tangential velocity of G^- with respect to G^+ at the GB.

The spherical GB rotates and shrinks without any shape change. This does not require any shape accommodation mechanism such as GB diffusion. We will therefore consider $\boldsymbol{h} = \boldsymbol{0}$. Assuming isotropic GB energy and defining $\boldsymbol{\theta} = \theta_1\boldsymbol{e}_1 + \theta_2\boldsymbol{e}_2 + \theta_3\boldsymbol{e}_3$ (the axial vector of $\boldsymbol{\Theta} - \boldsymbol{I}$) the dissipation inequality, given by (3.22), reduces to

$$V f_n + \boldsymbol{w} \cdot \tilde{\boldsymbol{f}}_\mathrm{t} \geq 0, \quad \text{where } f_n = \gamma\kappa \quad \text{and} \quad \tilde{\boldsymbol{f}}_\mathrm{t} = -\partial_{\boldsymbol{\theta}}\gamma. \tag{4.2}$$

Consequently, we postulate the following linear kinetic relations (see also [6]):

$$V = \mathcal{M} f_n + \mathcal{M}\tilde{\boldsymbol{\beta}} \cdot \tilde{\boldsymbol{f}}_{\mathrm{t}} \quad \text{and} \quad \boldsymbol{w} = \tilde{\boldsymbol{\beta}} V + \tilde{\boldsymbol{\mathcal{S}}} \tilde{\boldsymbol{f}}_{\mathrm{t}}, \tag{4.3}$$

where $\mathcal{M} > 0$ is the GB mobility, $\tilde{\boldsymbol{\beta}}$ is the coupling factor between rotational speed and normal GB velocity, and $\tilde{\boldsymbol{\mathcal{S}}}$ is the symmetric positive semi-definite sliding coefficient. Both the viscous effect and the twist characteristic of the GB are expected to contribute to the net sliding. To understand the physical meaning of the coefficients $\tilde{\boldsymbol{\beta}}$ and $\tilde{\boldsymbol{\mathcal{S}}}$, we take a cross-product of $(4.3)_2$ with $\boldsymbol{x}$ to obtain

$$\boldsymbol{V}_{\mathrm{t}} = \boldsymbol{\beta} V + \boldsymbol{\mathcal{S}} \boldsymbol{f}_{\mathrm{t}}, \quad \text{where} \tag{4.4}$$

$$\boldsymbol{\beta} = \boldsymbol{x} \times \tilde{\boldsymbol{\beta}}, \quad \boldsymbol{\mathcal{S}} \boldsymbol{f}_{\mathrm{t}} = \boldsymbol{x} \times \tilde{\boldsymbol{\mathcal{S}}} \tilde{\boldsymbol{f}}_{\mathrm{t}} \quad \text{and} \quad \boldsymbol{f}_{\mathrm{t}} = \left(\frac{1}{R}\right) \boldsymbol{e}_R \times \tilde{\boldsymbol{f}}_{\mathrm{t}}. \tag{4.5}$$

Equation $(4.5)_1$ relates $\tilde{\boldsymbol{\beta}}$ to the geometrical coupling factor $\boldsymbol{\beta}$ introduced in appendix A, whereas $(4.5)_2$ relates $\tilde{\boldsymbol{\mathcal{S}}}$ to the sliding coefficient $\boldsymbol{\mathcal{S}}$; the relation $(4.5)_3$ is motivated from the two-dimensional counterpart of the present discussion [6]. Next, we specialize these kinetic equations for a spherical GB, under various additional assumptions, and present analytical solutions wherever possible. When reduced to a two-dimensional setting, the derived relations will be identical to those obtained previously for a circular GB [1,6].

GB migration: when both geometrical coupling and GB sliding are negligible, kinetic equations $(4.3)_1$ and $(4.3)_2$ simplify to the well-known equations for curvature driven GB migration: $V = \mathcal{M}\gamma\kappa$ and $\boldsymbol{w} = \boldsymbol{0}$. Using $V = \dot{R}$ and $\kappa = -1/R$ (for a spherical GB), they can be solved to obtain $R(t) = \sqrt{R_0^2 - 2\mathcal{M}\gamma t}$ and $\boldsymbol{\theta}(t) = \boldsymbol{\theta}_0$, where R_0 is the initial GB radius and $\boldsymbol{\theta}_0$ is the initial misorientation. Both $\mathcal{M}$ and γ have been treated as constants.

Coupled motion without GB sliding: at temperatures far below the melting point, GB viscous sliding becomes negligible and geometrical coupling plays the dominant role in grain rotation [12]. The kinetic relations $(4.3)_1$ and $(4.3)_2$ then take the form $V = \mathcal{M}\gamma\kappa + \mathcal{M}\tilde{\boldsymbol{\beta}} \cdot \tilde{\boldsymbol{f}}_{\mathrm{t}}$ and $\boldsymbol{w} = \tilde{\boldsymbol{\beta}} V$, respectively. For a spherical GB, with $V = \dot{R}$ and $\boldsymbol{\beta} = (\boldsymbol{\Theta} - \boldsymbol{I})\boldsymbol{e}_R$ (see appendix A for the latter expression), $(4.5)_1$ and a cross-product of second kinetic relation with $\boldsymbol{x} = R\boldsymbol{e}_R$ furnishes $\boldsymbol{w} \times \boldsymbol{e}_R = -(\dot{R}/R)\boldsymbol{\theta} \times \boldsymbol{e}_R$ which on time integration gives $R(t)\boldsymbol{\theta}(t) = R_0\boldsymbol{\theta}_0$ for all ξ and ϕ. Note that we have used the same geometrical coupling factor associated with a planar GB for analysing the kinetics of a curved GB (see appendix A); this assumption is motivated from the two-dimensional atomistic studies where the geometrical coupling factor was observed to be same for planar and curved GBs (cf. [8] and the references therein). We use the isotropic energy of the form $\gamma = \gamma_0|\boldsymbol{\theta}|(A_c - \ln|\boldsymbol{\theta}|)$ (see §12.7 in [25]), where γ_0 and A_c are constants depending on the materials. Restricting ourselves to a spherical GB (for which $V = \dot{R}$, $\kappa = -1/R$, and $\tilde{\boldsymbol{\beta}} = -\boldsymbol{\theta}/R$), we eventually obtain $R(t) = (R_0^3 - 3\mathcal{M}\gamma_0 R_0|\boldsymbol{\theta}_0|t)^{1/3}$ and $\boldsymbol{\theta}(t) = R_0(R_0^3 - 3\mathcal{M}\gamma_0 R_0|\boldsymbol{\theta}_0|t)^{-1/3}\boldsymbol{\theta}_0$, where $\mathcal{M}$ has been treated as a constant.

Coupled motion without geometrical coupling: at temperatures close to the melting point, viscous sliding at the GB dominates over the geometrical coupling to govern grain rotation [12]. The kinetic relations $(4.3)_1$ and $(4.3)_2$ then reduce down to $V = \mathcal{M}\gamma\kappa$, and $\dot{\boldsymbol{\theta}} = \tilde{\boldsymbol{\mathcal{S}}}\tilde{\boldsymbol{f}}_{\mathrm{t}}$, respectively. If we assume $\tilde{\boldsymbol{\mathcal{S}}}$ and $\boldsymbol{\mathcal{S}}$ to be of the form $\tilde{\boldsymbol{\mathcal{S}}} = \tilde{\mathcal{S}}\boldsymbol{P}$ and $\boldsymbol{\mathcal{S}} = \mathcal{S}\boldsymbol{I}$, respectively, then $(4.5)_2$ requires $\tilde{\mathcal{S}} = \mathcal{S}/R^2$. Further manipulation yields the following implicit relation between R and $\boldsymbol{\theta}$:

$$R(\boldsymbol{\theta}) = R_0 \exp\left(\frac{\mathcal{M}}{\mathcal{S}}\{|\boldsymbol{\theta}|^2 - |\boldsymbol{\theta}_0|^2 + 2e^{2(A_c-1)}[E(1,u_0) - E(1,u)]\}\right), \tag{4.6}$$

where $u = 2(A_c - 1 - \ln|\boldsymbol{\theta}|)$, $u_0 = 2(A_c - 1 - \ln|\boldsymbol{\theta}_0|)$ and $E(n,y) = \int_y^\infty (e^{-u}/y^{1-n}u^n)du$ (the exponential integral); $\mathcal{M}$ and $\mathcal{S}$ have been considered to be constants.

Fully coupled motion: we finally consider the situation when both geometrical coupling and GB sliding will contribute comparable to the evolution of grain rotation. Assuming $\tilde{\boldsymbol{\mathcal{S}}}$ to be invertible, and eliminating $\tilde{f}_{\mathrm{t}}$ between $(4.3)_1$ and $(4.3)_2$, we derive

$$\dot{R} = -\frac{R}{R^2 + \mathcal{M}\boldsymbol{\theta}\cdot\tilde{\boldsymbol{\mathcal{S}}}^{-1}\boldsymbol{\theta}}(\mathcal{M}\gamma + \mathcal{M}\tilde{\boldsymbol{\mathcal{S}}}^{-1}\boldsymbol{\theta}\cdot\boldsymbol{w}). \tag{4.7}$$

An expression for $\boldsymbol{w}$ can be obtained by substituting $(4.3)_1$ in $(4.3)_2$

$$\boldsymbol{w} = \frac{\mathcal{M}\gamma\boldsymbol{\theta}}{R^2} + \left(\tilde{\boldsymbol{\mathcal{S}}} + \frac{\mathcal{M}}{R^2}\boldsymbol{\theta}\otimes\boldsymbol{\theta}\right)\tilde{f}_{\mathrm{t}}. \tag{4.8}$$

(c) Tricrystal

We consider a tricrystal, as shown in figure 2*c*, where grain G_1 is embedded inside a larger bicrystal made of two cubic grains G_2 and G_3. The tricrystal is subjected to external stress. The configuration has three GBs $\mathcal{S}_i$, with unit normals denoted by $\boldsymbol{n}_i$ $(i = 1, 2, 3)$, and a closed junction curve J. The normals are chosen such that both $\boldsymbol{n}_1$ and $\boldsymbol{n}_2$ point into G_1, whereas $\boldsymbol{n}_3$ points into G_2. In deriving the kinetic laws, we assume both the volumetric diffusion and the diffusion along the junction to be negligible. In addition, the magnitude of applied stresses are taken to be small enough, so that elastic and plastic deformation of the grains can be neglected. Under the combined effects of GB capillary force and the applied stress field the GBs will migrate, grain G_1 will rotate and translate (as a rigid body), grains G_2 and G_3 will translate rigidly relative to each other, and the junction J will move in space, all coupled to each other.

In the absence of defects within the grain, the orientation field associated with grain G_i, denoted by $\boldsymbol{R}_i$, will be homogeneous throughout the grain. We define the misorientation tensor for the respective GBs as $\boldsymbol{\Theta}_1 = \boldsymbol{R}_1^{\mathrm{T}}\boldsymbol{R}_2$, $\boldsymbol{\Theta}_2 = \boldsymbol{R}_1^{\mathrm{T}}\boldsymbol{R}_3$ and $\boldsymbol{\Theta}_3 = \boldsymbol{R}_2^{\mathrm{T}}\boldsymbol{R}_3$. We assume grains G_2 and G_3 to be non-rotating, thereby fixing their orientations once for all. As a result $\dot{\boldsymbol{\Theta}}_1\boldsymbol{\Theta}_1^{\mathrm{T}} = \dot{\boldsymbol{\Theta}}_2\boldsymbol{\Theta}_2^{\mathrm{T}} = -\dot{\boldsymbol{R}}_1\boldsymbol{R}_1^{\mathrm{T}}$. On the other hand, the velocities of rigidly deforming grains can be written as $\boldsymbol{v}_1 = \boldsymbol{w}\times\boldsymbol{x} + \dot{\boldsymbol{C}}_1$, $\boldsymbol{v}_2 = \dot{\boldsymbol{C}}_2$, $\boldsymbol{v}_3 = \boldsymbol{0}$, where $\boldsymbol{w}$ is the angular velocity of G_1 (the axial vector of $\dot{\boldsymbol{R}}_1\boldsymbol{R}_1^{\mathrm{T}}$) and $\boldsymbol{C}_i$ is the rigid translation of G_i (grain G_3 has been assumed to remain fixed). We define the relative translation velocity of adjacent grains at the respective GBs as $\dot{\boldsymbol{\mathcal{C}}}_1 = \dot{\boldsymbol{C}}_1 - \dot{\boldsymbol{C}}_2$, $\dot{\boldsymbol{\mathcal{C}}}_2 = \dot{\boldsymbol{C}}_1$, and $\dot{\boldsymbol{\mathcal{C}}}_3 = \dot{\boldsymbol{C}}_2$. Before we substitute these in the mass balance relations, we would additionally assume that the translational velocity of the embedded grain to be much smaller than its rotational velocity. We can justify this on the basis of the atomistic simulation results which do not show any significant translation in the absence of external stress [8]. The small amplitude of external stress considered here would therefore cause only small relative translation. Keeping this in mind, along with negligible diffusional fluxes in the grain, we use (3.3) to derive $\mathrm{div}^S\boldsymbol{h}_a = -\rho\boldsymbol{x}\times\boldsymbol{n}_a\cdot\boldsymbol{w}$ for $a = 1, 2$, and $\mathrm{div}^S\boldsymbol{h}_3 = -\rho\dot{\boldsymbol{\mathcal{C}}}_3\cdot\boldsymbol{n}_3$. These relations can be integrated and then combined with (3.4) (where $\boldsymbol{j} = \boldsymbol{0}$, $h_J = 0$, and ρ, v are non-singular at the junction) to obtain $\boldsymbol{h}_a = \boldsymbol{A}_a\boldsymbol{w}$ and $\boldsymbol{h}_3 = \boldsymbol{A}_3\dot{\boldsymbol{\mathcal{C}}}_3$, where $\boldsymbol{A}_i$ is a second-order tensor which depends on the geometry of $\mathcal{S}_i$ (see [2] for a similar calculation for a two-dimensional tricrystal). We also relate these fluxes to the chemical potential by assuming the Fick's law for superficial diffusion $\boldsymbol{h}_i = -\boldsymbol{D}_i\nabla^S\mu$ for $i = 1, 2, 3$ [15] where $\boldsymbol{D}_i$ is the (symmetric and tangential) diffusivity tensor along $\mathcal{S}_i$.

For the present case, the dissipation inequality in the bulk (3.21) is trivially satisfied. The dissipation inequalities at the GBs, given by (3.22), are however non-trivial and will be used in the following to derive the kinetic equations. Using Fick's law, and neglecting the terms of the order of $|\dot{\boldsymbol{\mathcal{C}}}_a|^2$ and $|\dot{\boldsymbol{R}}_a\dot{\boldsymbol{\mathcal{C}}}_a|$, we can reduce the inequalities to the form (no summation for repeated index i)

$$V_i f_i + \boldsymbol{w}\cdot\boldsymbol{\mathcal{G}}_i + \dot{\boldsymbol{\mathcal{C}}}_i\cdot\boldsymbol{\mathcal{H}}_i \geq 0 \quad \text{on } \mathcal{S}_i, \tag{4.9}$$

where $\boldsymbol{\mathcal{H}}_i = \boldsymbol{\sigma}\boldsymbol{n}_i$, $\boldsymbol{\mathcal{G}}_a = \boldsymbol{x}\times(\boldsymbol{\sigma}\boldsymbol{n}_a + \rho\mu\boldsymbol{n}_a) + \boldsymbol{A}_a^{\mathrm{T}}\boldsymbol{D}_a^{-1}\boldsymbol{A}_a\boldsymbol{w} + 2\boldsymbol{\Upsilon}_a$ and $\boldsymbol{\mathcal{G}}_3 = \boldsymbol{0}$. Here, $\boldsymbol{D}_i^{-1}$ is the Moore–Penrose pseudo-inverse of $\boldsymbol{D}_i$ which satisfies $\boldsymbol{D}_i^{-1}\boldsymbol{D}_i = \boldsymbol{D}_i\boldsymbol{D}_i^{-1} = \boldsymbol{P}_i$ [14], and $\boldsymbol{\Upsilon}_a$ is the axial vector associated with the skew part of $(\partial_{\boldsymbol{\Theta}_a}\gamma_a)\boldsymbol{\Theta}_a^{\mathrm{T}}$. Following Onsager, we use (4.9) to postulate linear

kinetic relations associated with $\mathcal{S}_a$ ($a=1,2$). In writing them, we assume the relative translational velocities $\dot{\boldsymbol{\mathcal{C}}}_a$ to be decoupled from GB migration and the rotation rate of grain G_1; a theory without this assumption can easily be constructed along similar lines. The kinetic relations are taken as

$$V_a = \mathcal{M}_a(f_a + \tilde{\boldsymbol{\beta}}_a \cdot \boldsymbol{\mathcal{G}}_a), \quad \boldsymbol{w} = \tilde{\boldsymbol{\beta}}_a V_a + \tilde{\boldsymbol{\mathcal{S}}}_a \boldsymbol{\mathcal{G}}_a, \quad \dot{\boldsymbol{\mathcal{C}}}_a = \boldsymbol{\mathcal{L}}_a \boldsymbol{\mathcal{H}}_a, \tag{4.10}$$

where the coefficients $\mathcal{M}_a$, $\tilde{\boldsymbol{\beta}}_a$ and $\tilde{\boldsymbol{\mathcal{S}}}_a$ have the same physical interpretation as described in §4b, and $\boldsymbol{\mathcal{L}}_a$ is the translational coefficient of the grains. Substituting $(4.10)_1$, $(4.10)_3$ and $(4.10)_2$ back into the dissipation inequality (4.9), we derive the following restrictions: $\mathcal{M}_a > 0$; $\tilde{\boldsymbol{\mathcal{S}}}_a$ and $\boldsymbol{\mathcal{L}}_a$ are symmetric positive semi-definite.

Furthermore, when sliding is active and $\tilde{\boldsymbol{\mathcal{S}}}_a$ is invertible, we can eliminate $\boldsymbol{\mathcal{G}}_a$ from $(4.10)_1$ with the help of $(4.10)_2$ to obtain

$$V_a = \frac{\mathcal{M}_a}{1 + \mathcal{M}_a \tilde{\boldsymbol{\beta}}_a \cdot \tilde{\boldsymbol{\mathcal{S}}}_a{}^{-1} \tilde{\boldsymbol{\beta}}_a} (f_a + \tilde{\boldsymbol{\beta}}_a \cdot \tilde{\boldsymbol{\mathcal{S}}}_a{}^{-1} \boldsymbol{w}). \tag{4.11}$$

We can also derive $(\boldsymbol{I} - \tilde{\boldsymbol{\mathcal{Z}}}_a \boldsymbol{A}_a^{\mathrm{T}} \boldsymbol{D}_a^{-1} \boldsymbol{A}_a)\boldsymbol{w} = \mathcal{M}_a f_a \tilde{\boldsymbol{\beta}}_a + \tilde{\boldsymbol{\mathcal{Z}}}_a(\boldsymbol{x}_a \times \boldsymbol{\sigma}\boldsymbol{n}_a + 2\boldsymbol{\Upsilon}_a + \rho\mu \boldsymbol{x}_a \times \boldsymbol{n}_a)$, where $\tilde{\boldsymbol{\mathcal{Z}}}_a = \tilde{\boldsymbol{\mathcal{S}}}_a + \mathcal{M}_a \tilde{\boldsymbol{\beta}}_a \otimes \tilde{\boldsymbol{\beta}}_a$. For an invertible $\tilde{\boldsymbol{\mathcal{S}}}_a$, we multiply both sides of this equation by $\tilde{\boldsymbol{\mathcal{Z}}}_a^{-1}$ and integrate the result over $\mathcal{S}_1$ and $\mathcal{S}_2$ for $a=1$ and $a=2$, respectively. The two expressions can be added to obtain the following expression for $\boldsymbol{w}$:

$$\boldsymbol{w} = \left(\sum_{a=1}^{2} \int_{\mathcal{S}_a} (\tilde{\boldsymbol{\mathcal{Z}}}_a^{-1} - \boldsymbol{A}_a^{\mathrm{T}} \boldsymbol{D}_a^{-1} \boldsymbol{A}_a) da \right)^{-1} \sum_{a=1}^{2} \int_{\mathcal{S}_a} (\mathcal{M}_a f_a \tilde{\boldsymbol{\mathcal{Z}}}_a^{-1} \tilde{\boldsymbol{\beta}}_a + \boldsymbol{x}_a \times \boldsymbol{\sigma}\boldsymbol{n}_a + 2\boldsymbol{\Upsilon}_a) da, \tag{4.12}$$

where we have used $\sum_{a=1}^{2} \int_{\mathcal{S}_a} \rho\mu \boldsymbol{x}_a \times \boldsymbol{n}_a da = \rho \int_{G_1} \boldsymbol{x} \times \nabla\mu dv = \boldsymbol{0}$ (recall that diffusional flux vanishes in the grain). To summarize the results obtained so far, we have the governing equations for the motion of $\mathcal{S}_1$ and $\mathcal{S}_2$ in (4.11), and the governing equation for rotation of G_1 in (4.12).

The kinetic relations for $\mathcal{S}_3$ can be derived similarly. In doing so, however, we allow translational velocity to be coupled with the normal motion. Starting with (4.9), and assuming linear kinetics, we obtain

$$\dot{\boldsymbol{\mathcal{C}}}_3 = \boldsymbol{\beta}_3 V_3 + \boldsymbol{\mathcal{L}}_3 \boldsymbol{\mathcal{H}}_3 \quad \text{and} \quad V_3 = \mathcal{M}_3(f_3 + \boldsymbol{\beta}_3 \cdot \boldsymbol{\mathcal{H}}_3), \tag{4.13}$$

where $\mathcal{M}_3 > 0$, $\boldsymbol{\beta}_3$, and $\boldsymbol{\mathcal{L}}_3$ (positive semi-definite) represent mobility, geometrical coupling factor and sliding coefficient, respectively, for $\mathcal{S}_3$. Replacing V_3 from $(4.13)_2$ in $(4.13)_1$ and integrating the final expression over $\mathcal{S}_3$ (because the translational velocities are homogeneous), we write

$$\dot{\boldsymbol{\mathcal{C}}}_3 = \int_{\mathcal{S}_3} (\mathcal{M}_3 f_3 \boldsymbol{\beta}_3 + \boldsymbol{\mathcal{Z}}_3 \boldsymbol{\mathcal{H}}_3) da, \tag{4.14}$$

where the outer grains have been assumed to be much larger than the embedded grain, and hence, the contribution coming from the integration over the periphery of G_1 has been neglected.

On the other hand, the governing equation for average translation velocity of the embedded grain can be obtained by first integrating $(4.10)_3$ for $a=1$ and 2, respectively, and then adding them to obtain

$$\dot{\mathcal{C}}_1 = \frac{1}{\mathrm{area}(\mathcal{S}_1 \cup \mathcal{S}_2)} \left(\mathrm{area}(\mathcal{S}_1) \dot{\boldsymbol{\mathcal{C}}}_3 + \sum_{a=1}^{2} \int_{\mathcal{S}_a} \boldsymbol{\mathcal{L}}_a \boldsymbol{\mathcal{H}}_a da \right), \tag{4.15}$$

where $\dot{\boldsymbol{\mathcal{C}}}_3$ is given by (4.14). In $(4.13)_2$ we have the governing equation for the normal motion of $\mathcal{S}_3$ and in (4.15) for the translation of the embedded grain.

Finally, we derive the kinetic relations which govern junction dynamics. For negligible diffusion along the junction curve, the dissipation inequality (3.27) simplifies to $\boldsymbol{\mathcal{F}}_J \cdot \boldsymbol{q}_p \geq 0$. Assuming linear kinetics we postulate that

$$\boldsymbol{q}_p = \boldsymbol{\mathcal{M}}_J \boldsymbol{\mathcal{F}}_J, \tag{4.16}$$

where $\boldsymbol{\mathcal{M}}_J$ is the positive semi-definite junction mobility tensor. An analogous treatment in a two-dimensional setting can be seen in [30] (see also [2]). The junction force $\boldsymbol{\mathcal{F}}_J$ given by (3.28)

is a function of the unknown local orientations of the adjacent GBs which, for a non-splitting junction, can be calculated using the compatibility conditions $V_i = \boldsymbol{q}_p \cdot \boldsymbol{n}_i$ (see [2,30] for a detailed calculation in two-dimension).

To conclude, the complete set of kinetic equations governing the coupled GB motion in the tricrystalline arrangement includes (4.11) for the motion of $\mathcal{S}_1$ and $\mathcal{S}_2$, $(4.13)_2$ for the motion of $\mathcal{S}_3$, (4.12) for the rotation of the embedded grain G_1 (the outer grains are non-rotating) (4.15) and (4.14) for the translation of grains G_1 and G_2, respectively (whereas grain G_3 is stationary), and (4.16) (in association with the compatibility condition) for the motion of the junction curve.

5. Concluding remarks

We have presented a thermodynamically consistent three-dimensional study of coupled GB motion in the presence of junctions, hitherto restricted to two-dimensional crystalline materials. Towards this end, we introduced a novel continuum mechanics-based theory of irreversible dynamics of incoherent interfaces with junctions, which allows for diffusion in the bulk, on the interface, and along the junction curve. The various local dissipation inequalities derived therein were used to motivate kinetic relations for the coupled GB motion in two bicrystals and one tricrystal. These relations were solved analytically whenever it was possible to do so, but were otherwise left in a form amenable to numerical computations. In any case, the results clearly demonstrated the effect of coupling on the grain dynamics. Consider for instance the shrinking of an isolated grain, embedded within a larger grain, under the action of capillary. Without coupling, the embedded grain can disappear only by shrinking to a vanishing size. However with coupling, the grain can disappear by aligning its orientation with the outer grain even before it has shrunk significantly [6]. The proposed kinetic relations also emphasize the coupling of junction dynamics with both grain and GB motion. Depending on the junction mobility, grain dynamics can experience a substantial drag compared with the case with no junctions [2].

This work can form a basis for research in several future directions. The theory of incoherent interfaces, which includes junctions and diffusion, is in fact applicable to a more general situation where the grains are allowed to deform plastically. The resulting framework would be useful for phenomena which involves coupling of plastically deforming bulk with moving incoherent interfaces and junctions [31]. Second, the kinetic relations derived for the tricrystal can be used to study the coupled motion in polycrystalline materials containing large number of grains and junctions. Of course, this will demand significant computational effort and hence efficient numerical algorithms. A related direction of work would be to develop numerical techniques (such as level set methods) for solving equations of coupled motion of an embedded grain with anisotropic constitutive properties. Third, the computation of the vectorial coupling factor, which has been restricted here to small angle GBs, should be extended to large angle GBs. Finally, three-dimensional atomistic simulations will be required to clarify the nature of various kinetic coefficients (including the coupling factor), in particular, regarding their dependence on three misorientation angles and two orientation angles of the GB.

Data accessibility. This research involves no data.

Acknowledgements. We thank anonymous reviewers for their constructive comments which led to considerable improvement in the manuscript.

Funding statement. Neither author received funding to carry out this research.

Author contributions. A.G. planned the research. A.B. conducted the research, and worked out all the derivations and examples. Both A.G. and A.B. analysed the results and contributed equally to the writing.

Appendix A. Geometrical coupling factor

During the migration of a tilt or a mixed GB, the adjacent grains undergo a tangential motion giving rise to a coupled dynamics (ch. 14 in [25], and [7,12,29]). The deformation of the grain in the wake of a moving GB, during coupled motion, is essentially controlled by the intrinsic edge dislocation content at the GB. Screw dislocations, if present, just glide along the GB plane

and contribute only to grain sliding without affecting the coupling process [7]. For a moving planar symmetric tilt GB, whose wake experiences a simple shear deformation, Cahn *et al.* [12] introduced *geometrical coupling factor* as the ratio of the relative tangential velocity (in the absence of viscous sliding) to the GB velocity. For a large misorientation range of a symmetric tilt boundary, containing single array of edge dislocations, the coupling factor (denoted by β) was calculated to be $\beta = 2\tan(\theta/2)$, where θ is the misorientation angle. This was later verified both in experiments and atomistic simulations [13,29]. In general, however, most of the GBs are mixed, containing multiple sets of edge and screw dislocation arrays. If the above definition of the geometrical coupling factor is generalized to an arbitrary GB, the result will be a vector given by

$$\boldsymbol{\beta} = \frac{\boldsymbol{P}[\![\boldsymbol{v}]\!]}{V}. \tag{A 1}$$

We will now use this definition to derive an expression for the coupling factor for several special cases, all with planar GBs such as shown in figure 2*a*.

Symmetric tilt GB: let $\boldsymbol{F}$ be the total deformation gradient of the grains with respect to a fixed reference configuration. Compatibility at the boundary requires $[\![\boldsymbol{F}]\!] = \boldsymbol{a} \otimes \boldsymbol{n}_r$ and $[\![\boldsymbol{v}]\!] = -V_r\boldsymbol{a}$, where $\boldsymbol{a}$ is an arbitrary vector, whereas $\boldsymbol{n}_r$ and V_r, respectively, are the normal vector and the normal velocity of the GB in the reference configuration. Without loss of generality, we can assume that $\boldsymbol{F}^+ = \boldsymbol{I}$ and $\boldsymbol{v}^+ = \boldsymbol{0}$. Consequently, $\boldsymbol{n}_r = \boldsymbol{n}$ and $V_r = V$ [14]. On the other hand, the multiplicative decomposition of $\boldsymbol{F}$, under the present assumption of elastically rigid grains, takes the form $\boldsymbol{F} = \boldsymbol{R}\boldsymbol{F}^p$ [14], where $\boldsymbol{R}$ is the lattice rotation tensor and $\boldsymbol{F}^p$ is the plastic deformation gradient. If we assume the plastic deformation to be isochoric ($\det\boldsymbol{F}^p = 1$), and that $\boldsymbol{F}^{p+} = \boldsymbol{I}$, then the above considerations lead to $\boldsymbol{F}^- = \boldsymbol{I} + \boldsymbol{\beta} \otimes \boldsymbol{n}$, where $\boldsymbol{\beta} = -\boldsymbol{P}\boldsymbol{a}$ is a tangential vector (the superscript 'minus sign' will be suppressed hereafter). The total Burgers vector $\boldsymbol{B}$ of all the GB dislocations cut by a unit vector $\boldsymbol{p}$ lying on the GB plane is given by the Frank–Bilby equation $\boldsymbol{B} = (\boldsymbol{I} - \boldsymbol{R}^{\mathrm{T}})\boldsymbol{p} = (\boldsymbol{I} - \boldsymbol{F}^p)\boldsymbol{p}$ [14]. Assuming all the edge dislocations at the GB to glide in a single slip direction, we can write the resulting plastic distortion rate as $\dot{\boldsymbol{F}}^p(\boldsymbol{F}^p)^{-1} = \dot{\zeta}\,\boldsymbol{s} \otimes \boldsymbol{m}$ (cf. ch. 106 in [32]), where $\dot{\zeta}$, $\boldsymbol{s}$ and $\boldsymbol{m}$ stand for slip rate, unit slip vector and unit normal to the slip plane, respectively ($\boldsymbol{s}$ and $\boldsymbol{m}$ are mutually perpendicular). With initial values of ζ and $\boldsymbol{F}^p$ as 0 and $\boldsymbol{I}$, respectively, time integration of the evolution equation yields $\boldsymbol{F}^p = \exp(\zeta(t)\boldsymbol{s} \otimes \boldsymbol{m})(\boldsymbol{F}^p|_{t=0}) = \boldsymbol{I} + \zeta\,\boldsymbol{s} \otimes \boldsymbol{m}$. If the orientation of grain G^- is related to that of G^+ by an anticlockwise rotation of angle θ_3 about $\boldsymbol{e}_3$-axis, then we can write $\boldsymbol{R} = \cos\theta_3(\boldsymbol{e}_1 \otimes \boldsymbol{e}_1 + \boldsymbol{e}_2 \otimes \boldsymbol{e}_2) + \sin\theta_3(\boldsymbol{e}_2 \otimes \boldsymbol{e}_1 - \boldsymbol{e}_1 \otimes \boldsymbol{e}_2) + \boldsymbol{e}_3 \otimes \boldsymbol{e}_3$. Using this in the Frank–Bilby equation for $\boldsymbol{p} = \boldsymbol{e}_2$, and recalling that $\boldsymbol{B} = |\boldsymbol{B}|\boldsymbol{s}$, we obtain $|\boldsymbol{B}| = 2\sin(\theta_3/2)$ and $\boldsymbol{s} = -\cos(\theta_3/2)\boldsymbol{e}_1 + \sin(\theta_3/2)\boldsymbol{e}_2$ (and hence $\boldsymbol{m} = -\sin(\theta_3/2)\boldsymbol{e}_1 - \cos(\theta_3/2)\boldsymbol{e}_2$). Finally, with the help of expressions derived above for total and plastic deformation gradients, we can obtain $\zeta = -|\boldsymbol{B}|/(\boldsymbol{m} \cdot \boldsymbol{e}_2)$ and consequently, $\boldsymbol{\beta} = 2\tan(\theta_3/2)\boldsymbol{e}_2$. This expression for the coupling factor was derived earlier by Cahn *et al.* [12]. For small misorientation angle, the coupling factor takes a simple form $\boldsymbol{\beta} = \theta_3\boldsymbol{e}_2$ (ch. 14 in [25]).

General tilt boundary with small misorientation: restricting ourselves to small misorientation, we consider a tilt GB such that $\boldsymbol{R} = \boldsymbol{I} + \theta_2(\boldsymbol{e}_2\times) + \theta_3(\boldsymbol{e}_3\times)$, where $(\boldsymbol{e}\times)$ represents a skew tensor with components given by $(\boldsymbol{e}\times)_{jk} = \varepsilon_{jlk}e_l$ (here ε_{jlk} is the permutation symbol). In other words, grain G^- is obtained by rotating the reference grain G^+ anticlockwise about $\boldsymbol{e}_2$ and $\boldsymbol{e}_3$ by small angles θ_2 and θ_3, respectively. The dislocation density tensor at the GB, defined as $\boldsymbol{\alpha} = (\boldsymbol{I} - \boldsymbol{F}^p)(\boldsymbol{n}\times) = (\boldsymbol{I} - \boldsymbol{R}^{\mathrm{T}})(\boldsymbol{n}\times)$ [14,33], takes the form $\boldsymbol{\alpha} = \theta_2\boldsymbol{e}_1 \otimes \boldsymbol{e}_2 + \theta_3\boldsymbol{e}_1 \otimes \boldsymbol{e}_3$. This represents two arrays of edge dislocations having line direction along $\boldsymbol{e}_2$ and $\boldsymbol{e}_3$, and slip direction $\boldsymbol{e}_1$, with densities θ_2 and θ_3, respectively. To calculate the geometrical coupling factor, we exploit linearity in extending the result for a symmetric tilt boundary to the present situation to obtain $\boldsymbol{\beta} = \theta_3\boldsymbol{e}_2 - \theta_2\boldsymbol{e}_3$. The coupling factor, therefore, has contributions from both arrays of edge dislocations.

Twist GB with small misorientation: we now consider a twist GB with small misorientation such that the grain G^- is rotated by an anticlockwise angle θ_1, about $\boldsymbol{e}_1$-axis, with respect to grain G^+. For small angle, we can write $\boldsymbol{R} = \boldsymbol{I} + \theta_1(\boldsymbol{e}_1\times)$. As a result $\boldsymbol{\alpha} = -\theta_1(\boldsymbol{e}_2 \otimes \boldsymbol{e}_2 + \boldsymbol{e}_3 \otimes \boldsymbol{e}_3)$, which represents two arrays of screw dislocations (both with density θ_1) with line directions parallel to $\boldsymbol{e}_2$ and $\boldsymbol{e}_3$. With this in mind, we assume the plastic deformation gradient as $\boldsymbol{F}^p = \boldsymbol{I} + \zeta(\boldsymbol{s}_1 \otimes \boldsymbol{m}_1 + \boldsymbol{s}_2 \otimes \boldsymbol{m}_2)$,

where we have considered two mutually orthogonal slip systems with equal slip magnitude, such that $|\boldsymbol{s}_1| = |\boldsymbol{s}_2| = |\boldsymbol{m}_1| = |\boldsymbol{m}_2| = 1$ and $\boldsymbol{s}_1 \cdot \boldsymbol{s}_2 = \boldsymbol{s}_1 \cdot \boldsymbol{m}_1 = \boldsymbol{s}_2 \cdot \boldsymbol{m}_2 = \boldsymbol{m}_1 \cdot \boldsymbol{m}_2 = 0$. On the other hand, the total deformation gradient is of the form considered above, i.e. $\boldsymbol{F} = \boldsymbol{I} + \boldsymbol{\beta} \otimes \boldsymbol{e}_1$. With the assumption of small deformation and small misorientation, the multiplicative decomposition of the deformation gradient becomes an additive decomposition so as to yield $\boldsymbol{\beta} \otimes \boldsymbol{e}_1 = \theta_1(\boldsymbol{e}_1 \times) + \zeta(\boldsymbol{s}_1 \otimes \boldsymbol{m}_1 + \boldsymbol{s}_2 \otimes \boldsymbol{m}_2)$. Projecting this onto $\boldsymbol{e}_1$, $\boldsymbol{e}_2$ and $\boldsymbol{e}_3$, we obtain $\boldsymbol{\beta} = \zeta(\boldsymbol{s}_1(\boldsymbol{m}_1 \cdot \boldsymbol{e}_1) + \boldsymbol{s}_2(\boldsymbol{m}_2 \cdot \boldsymbol{e}_1))$, and $\boldsymbol{s}_1 \cdot \boldsymbol{e}_1 = \boldsymbol{s}_2 \cdot \boldsymbol{e}_1 = 0$, $\boldsymbol{m}_1 = \boldsymbol{s}_2$ and $\boldsymbol{m}_2 = \boldsymbol{s}_1$. These results immediately furnish $\boldsymbol{\beta} = \boldsymbol{0}$. We have therefore shown that the geometrical coupling factor for a twist boundary (with small misorientation) is zero, hence confirming the qualitative arguments provided in [1,7,12].

A cubic grain embedded in a large grain: as an application of the results obtained above, we now consider an example where a cubic grain (whose edges are aligned with directions $\boldsymbol{e}_1$, $\boldsymbol{e}_2$ and $\boldsymbol{e}_3$) is embedded inside another grain such that the (infinitesimal) misorientation between them is given by $\boldsymbol{R} = \boldsymbol{I} + \theta_1(\boldsymbol{e}_1 \times) + \theta_2(\boldsymbol{e}_2 \times) + \theta_3(\boldsymbol{e}_3 \times)$. The surface dislocation density tensor for the GB with normal $\boldsymbol{e}_1$ can be calculated as $\boldsymbol{\alpha} = -\theta_1(\boldsymbol{e}_2 \otimes \boldsymbol{e}_2 + \boldsymbol{e}_3 \otimes \boldsymbol{e}_3) + \theta_2 \boldsymbol{e}_1 \otimes \boldsymbol{e}_2 + \theta_3 \boldsymbol{e}_1 \otimes \boldsymbol{e}_3$; the GB is of a mixed type consisting of two mutually perpendicular sets of edge dislocations (with densities θ_2 and θ_3) and two mutually perpendicular sets of screw dislocations (both with densities θ_1). The dislocation content at other boundaries can be obtained in a similar manner. In evaluating the geometrical coupling factor associated with the boundary with normal $\boldsymbol{e}_1$, we exploit linearity in our arguments (owing to small misorientation) to combine the results obtained above for tilt and twist boundaries to write $\boldsymbol{\beta}_{\boldsymbol{e}_1} = \theta_3 \boldsymbol{e}_2 - \theta_2 \boldsymbol{e}_3$. We can similarly calculate the coupling factors for the GBs with normal $\boldsymbol{e}_2$ and $\boldsymbol{e}_3$ as $\boldsymbol{\beta}_{\boldsymbol{e}_2} = -\theta_3 \boldsymbol{e}_1 + \theta_1 \boldsymbol{e}_3$, and $\boldsymbol{\beta}_{\boldsymbol{e}_3} = \theta_2 \boldsymbol{e}_1 - \theta_1 \boldsymbol{e}_2$, respectively. It is easily verifiable that $\boldsymbol{\beta}_{-\boldsymbol{e}_1} = -\boldsymbol{\beta}_{\boldsymbol{e}_1}$, etc., where $\boldsymbol{\beta}_{-\boldsymbol{e}_1}$ represents the coupling factor associated with the face with normal $-\boldsymbol{e}_1$.

References

1. Cahn JW, Taylor JE. 2004 A unified approach to motion of grain boundaries, relative tangential translation along grain boundaries, and grain rotation. *Acta Mater.* **52**, 4887–4898. (doi:10.1016/j.actamat.2004.02.048)
2. Basak A, Gupta A. In press. Simultaneous grain boundary motion, grain rotation, and sliding in a tricrystal. *Mech. Mater.* (doi:10.1016/j.mechmat.2015.01.012)
3. Koch CC, Ovid'ko IA, Seal S, Veprek S. 2007 *Structural nanocrystalline materials: fundamentals and applications*. New York, NY: Cambridge University Press.
4. Wang L, Teng J, Liu P, Hirata A, Ma E, Zhang Z, Chen M, Han X. 2014 Grain rotation mediated by grain boundary dislocations in nanocrystalline platinum. *Nat. Commun.* **5**, 1–7. (doi:10.1038/ncomms5402)
5. Taylor JE, Cahn JW. 2007 Shape accomodation of a rotating embedded crystal via a new variational formulation. *Interfaces Free Bound.* **9**, 493–512. (doi:10.4171/IFB/174)
6. Basak A, Gupta A. 2014 A two-dimensional study of coupled grain boundary motion using the level set method. *Model. Simul. Mater. Sci. Eng.* **22**, 055022. (doi:10.1088/0965-0393/22/5/055022)
7. Gorkaya T, Molodov KD, Molodov DA, Gottstein G. 2011 Concurrent grain boundary motion and grain rotation under an applied stress. *Acta Mater.* **59**, 5674–5680. (doi:10.1016/j.actamat.2011.05.042)
8. Trautt ZT, Mishin Y. 2014 Capillary-driven grain boundary motion and grain rotation in a tricrystal: a molecular dynamics study. *Acta Mater.* **65**, 19–31. (doi:10.1016/j.actamat.2013.11.059)
9. Simha NK, Bhattacharya K. 2000 Kinetics of phase boundaries with edges and junctions in a three-dimensional multi-phase body. *J. Mech. Phys. Solids* **48**, 2619–2641. (doi:10.1016/S0022-5096(00)00008-9)
10. Capriz G, Mariano PM. 2004 Balance at a junction among coherent interfaces in materials with substructure. In *Advances in multifield theories for continua with substructure* (eds G Capriz, PM Mariano), pp. 243–263. New York, NY: Springer Science.
11. Cermelli P, Gurtin ME. 1994 The dynamics of solid-solid phase transitions 2. Incoherent interfaces. *Arch. Ration. Mech. Anal.* **127**, 41–99. (doi:10.1007/BF01845217)

12. Cahn JW, Mishin Y, Suzuki A. 2006 Coupling grain boundary motion to shear deformation. *Acta Mater.* **54**, 4953–4975. (doi:10.1016/j.actamat.2006.08.004)
13. Cahn JW, Mishin Y, Suzuki A. 2006 Duality of dislocation content of grain boundaries. *Phil. Mag.* **86**, 3965–3980. (doi:10.1080/14786430500536909)
14. Gupta A, Steigmann DJ. 2012 Plastic flow in solids with interfaces. *Math. Methods Appl. Sci.* **35**, 1799–1824. (doi:10.1002/mma.1611)
15. Gurtin ME, Jabbour ME. 2002 Interface evolution in three dimensions with curvature-dependent energy and surface diffusion: interface-controlled evolution, phase transitions, epitaxial growth of elastic films. *Arch. Ration. Mech. Anal.* **163**, 171–208. (doi:10.1007/s00205020193)
16. dell'Isola F, Seppecher P, Madeo A. 2012 How contact interactions may depend on the shape of Cauchy cuts in Nth gradient continua: approach "*à la D'Alembert*". *Zeit. für ang. Math. Phys.* **63**, 1119–1141. (doi:10.1007/s00033-012-0197-9)
17. Fried E, Gurtin ME. 2004 A unified treatment of evolving interfaces accounting for small deformations and atomic transport with emphasis on grain-boundaries and epitaxy. *Adv. Appl. Mech.* **40**, 1–177. (doi:10.1016/S0065-2156(04)40001-5)
18. dell'Isola F, Romano A. 1987 On the derivation of thermomechanical balance equations for continuous systems with a nonmaterial interface. *Int. J. Eng. Sci.* **25**, 1459–1468. (doi:10.1016/0020-7225(87)90023-1)
19. dell'Isola F, Kosinski W 1991 The interfaces between phases as a layer. II. A H-order model for two dimensional nonmaterial continua. In *Proc. of Vth Int. Meeting on Waves and Stability in Continuous Media, Sorrento, Italy, October 1989*.
20. Giaquinta M, Hildebrandt S. 2004 *Calculus of variations* (*in two volumes*). Berlin, Germany: Springer.
21. Gurtin ME. 2000 *Configurational forces as basic concepts of continuum physics*. New York, NY: Springer.
22. Maugin GA. 1995 Material forces: concepts and applications. *Appl. Mech. Rev.* **48**, 213–245. (doi:10.1115/1.3005101)
23. Mariano PM. 2013 Covariance in plasticity. *Proc. R. Soc. A* **469**, 20130073. (doi:10.1098/rspa.2013.0073)
24. Mariano PM. 2014 Mechanics of material mutations. *Adv. Appl. Mech.* **47**, 1–91. (doi:10.1016/B978-0-12-800130-1.00001-1)
25. Read WT. 1953 *Dislocations in crystals*. New York, NY: McGraw-Hill.
26. Herring C. 1951 Surface tension as a motivation for sintering. In *The physics of powder metallurgy* (ed. WE Kingstion), pp. 143–179. New York, NY: McGraw-Hill.
27. Onsager L. 1931 Reciprocal relations in irreversible processes. I. *Phys. Rev.* **37**, 405–426. (doi:10.1103/PhysRev.37.405)
28. Truesdell C. 1984 *Rational thermodynamics*. New York, NY: Springer.
29. Molodov DA, Ivanov VA, Gottstein G. 2007 Low angle tilt boundary migration coupled to shear deformation. *Acta Mater.* **55**, 1843–1848. (doi:10.1016/j.actamat.2006.10.045)
30. Fischer FD, Svoboda J, Hackl K. 2012 Modelling the kinetics of a triple junction. *Acta Mater.* **60**, 4704–4711. (doi:10.1016/j.actamat.2012.05.018)
31. Basak A, Gupta A. Submitted. Plasticity in multi-phase solids with incoherent interfaces and junctions.
32. Gurtin ME, Fried E, Anand L. 2010 *The mechanics and thermodynamics of continua*. New York, NY: Cambridge University Press.
33. Gurtin ME. 2008 A theory of grain boundaries that accounts automatically for grain misorientation and grain boundary orientation. *J. Mech. Phys. Solids* **56**, 640–662. (doi:10.1016/j.jmps.2007.05.002)